East African Scholars Multidisciplinary Bulletin
Abbreviated Key Title: East African Scholars Multidiscip Bull
ISSN 2617-4413 (Print) | ISSN 2617-717X (Online)
Published By East African Scholars Publisher, Kenya

Volume-6 | Issue-1 | Feb-2023 | DOI: 10.36349/easjmb.2023.v06i01.001

Original Research Article

Green Synthesis of Nb_2O_5 Nanoparticles and Photodegradation of Remazol Yellow RR Dye

M. J. Pawar[1*], M. D. Gaonar[1], A. D. Khajone[1], P. R. Malasane[2]

[1]Laboratory of Materials Synthesis, Department of Chemistry, Smt. Narsamma Arts, Commerce and Science College, Amravati, M. S. India
[2]Department of Chemistry, Sipna College of Engineering and Technology, Amravati M. S. India

Article History
Received: 03.01.2023
Accepted: 09.02.2023
Published: 28.02.2023

Journal homepage:
https://www.easpublisher.com

Quick Response Code

Abstract: Synthesis of nanoparticles by the recently developed green approach is extremely promising because of its non-toxicity and environmentally friendly nature. In present investigation, Nb_2O_5 nanoparticles were prepared by environmental friendly way from niobium ethaoxide using Aloe Vera leaf pulp. The synthesis of Nb_2O_5 nanoparticles was confirmed by systematic characterization using XRD, EDX, Brunauer–Emmett–Teller (BET) surface area measurements and FTIR studies. The removal efficiency of Remazol yellow RR dye over the as synthesized Nb_2O_5 nanoparticles as a photocatalyst was determined along with emphasizing on the parameters of initial dye concentration, catalyst loading and pH. For the photocatalytic degradation of Remazol yellow RR dye solutions pH was varied in the range of 2 to 9. For the optimization, the maximum decolorization of 95 % was observed in 120 min for low initial dye concentration of 30 mg/L for 1.5 g/L of Nb_2O_5 photocatalyst. Besides, the effects of oxidant species and scavengers were studied systematically.

Keywords: Green synthesis; Nb2O5; Remazol Yellow RR dye; Photocatalysis.

1. INTRODUCTION

Water is necessary for life and a valuable resource for civilization; it also plays an important role in natural ecosystems and climate regulation. The use of photocatalysts for wastewater recycling could be a solution to many countries' long-standing freshwater shortages [1]. Wastewater from the pulp, leather, fabric, polymer, pesticide and pharmaceutical sectors comprises a variety of organic contaminants, including dyes that contaminate water and harmful life on the planet [2-4]. Separating and degrading these organic waste products has taken precedence in ensuring a nontoxic and pollution-free environment [5].

Heterogeneous photocatalysis is one of the best methods to remove color contaminants from water without forming any hazardous by-products. This process is based on the activation of semiconductor materials (like TiO_2, ZnO, Fe_2O_3, Nb_2O_5 etc.) by solar or artificial light irradiation. Among the semiconductor-based photocatalysts, Niobium materials are promising materials as photocatalysts and solid acid catalysts, thus has been widely applied in different kinds of fields [6-8]. Niobium pentoxide (Nb_2O_5) is recently most studied semiconductor in photocatalysis due to its chemical and physical properties, availability, and non-toxicity. However, because of its large bandgap energy (E_g= 3.1 – 4.0 eV). Niobium oxide (Nb_2O_5) has a wide range of catalytic activities for various reactions including dehydration, hydration, dehydrogenation, and many types of oxidation reactions [9-11]. Nb_2O_5 shows a great promise in providing strong surface acidity and stability in aqueous medium for various acid-catalyzed reactions. In addition, pure or doped Nb_2O_5 are the focuses of growing attention for the photo-degradation of organic contaminants [12, 13]. Particularly, the preparations of Nb_2O_5 with different nanostructures and morphologies by chemical synthesis could enable detailed elucidation of structure-activity relationships.

Green synthesis of nanoparticles has gotten more publicity, because of its low cost, simplicity, scalability, eco-friendliness, and the wide range of metabolites secreted by plants. Plant products such as leaves, bark, roots, stems, peels, and other biological resources are accessible in nature and could be used for the green production of nontoxic nanoparticles. Plant extract contains various phytochemicals such as

***Corresponding Author:** M. J. Pawar
Laboratory of Materials Synthesis, Department of Chemistry, Smt. Narsamma Arts, Commerce and Science College, Amravati, M. S. India

polyphenols, flavonoids, terpenoids, phenolic acids, which are responsible for the reduction and formation of stabilized nanoparticles [12]. The goal of this study was to synthesize the Nb_2O_5 nanoparticles by using Aloe Vera leaves pulp as reducing/stabilizing agent and studying its photocatalytic efficiency for the degradation of reactive azo dye (Remazol yellow RR dye).

2. EXPERIMENTAL

2.1 Green synthesis of Nb_2O_5 nanoparticles

Analytical grade niobium ethaoxide, 2-propanol and ammonia solution were purchased from Merck, India. All chemicals are used without further purification. The Aloe Vera leaves were collected from the campus of Smt. Narsamma Arts, Commerce and Science College, Amravati M.S. India. The fresh leaves were then washed multiple times with tap water followed by deionized water. The leaves were then peeled off to get the transparent pulp mass from the leaves. The obtained pulp was dissolved in 2-propanol in calculated quantity.

Niobium ethaoxide was used as the precursor for the synthesis of the Nb_2O_5 nanoparticles. The calculated quantity of 50 mL of the solution of Aloe Vera jelly in 2-prpanol was added dropwise to the 50 mL of 2M niobium ethaoxide solution in 1:1 ratio at room temperature. Following this, 1 M ammonia solution was added till the pH became 9. The resultant mixture was stirred at 5000 rpm using a magnetic stirrer for 120 min and the formation of intense creamy colored solution was transferred to china dish and was left at room temperature for 5 h. It was followed by the calcination at 450 (sample coded as Nb-A) and 500˚C (sample coded as Nb-B) for 3 h. After calcination, the obtained nanoparticles were cleansed by subsequent washing with ethanol and water for 3–4 times. The Nb_2O_5 nanoparticles were finally dried in a hot air oven at 90˚C for 5 h and stored at dry place for further use.

2.2 Characterization

XRD patterns of the synthesized Nb_2O_5 samples were obtained using a Rigaku diffractometer using Cu-$K\alpha$ as a source of radiation. The UV-VIS spectra of the sample to measure the absorbance of the dye which were done by using the double beam UV-1700 Series Spectrophotometer (Shimadzu corporation, Japan). PL spectra of the catalysts were recorded using a PerkinElmer spectrophotometer. The morphology of nanoparticles was analyzed by means of field emission scanning electron microscope (JEOL JSM-7600F, Japan) run at a voltage of 5.0 KV. BET surface area assessment was performed using a Smart Sorb 92/93 surface area analyzer.

2.3 Photocatalytic activity

The photocatalytic degradation experiments were performed with a photocatalytic reactor containing a round and hollow Pyrex glass vessel with 1.0 L limit, 10 cm breadth and 15 cm stature. Mercury light of 100 W was placed in a 5 cm width quartz tube with one end firmly fixed by a Teflon plug. The light and the tube were then submerged in the photoreactor cell. The temperature of entire reactor was kept at 25˚C using continuous water flow system around the glass vessel of reactor.

To study the photocatalytic activity of Nb_2O_5 nanoparticles, a series of RR dye solution with different concentrations 10 to 50 ppm were prepared. 150 ml of the dye solution was taken in a beaker along with different quantity of Nb_2O_5 samples; 0.5 to 2.0 g/L and kept under UV-light along with continuous stirring at room temperature to maintain the uniformity over the span of reaction. The spectrophotometric analysis of dyes before and after the irradiation was utilized to measure the decolorization efficiency of dyes.

The absorbance of dyes was measured by using UV–Vis spectrophotometer at the wavelengths of maximum absorbance of dye. The decreasing absorbance of dye at the wavelengths of absorbance maximum after the visible light irradiation shows the decolorization rate of dye. The degradation efficiency of the dye has been calculated as shown in Eq. I.

$$\% \text{ Degradation} = \frac{C_O - C_t}{C_O} \times 100 \text{ ………. (Eq. I)}$$

Where C_o is the initial dye concentration and C_t is the dye concentration after time t.

3. RESULTS AND DISCUSSION

As synthesized Nb_2O_5 samples were characterized by XRD, EDAX, N_2 adsorption-desorption analysis, UV-visible spectra, FT-IR techniques and TEM analysis.

3.1 XRD analysis

To understand the phase purity of the prepared materials, XRD analysis was performed and is shown in Figure 1. A preliminary study at calcination temperatures 450˚C and 500˚C as in Figure demonstrate that after heating at 450°C the samples remain amorphous. Only on reaching temperatures higher than 500°C can the main signals of different niobium crystal phases be detected. All the diffraction patterns correspond to the pure crystalline hexagonal Nb_2O_5 phase (JCPDS no. 28-0317) and no possible impurity phase was found in the samples. The predominant peak of Nb_2O_5 at 2θ=28.52˚ corresponding to the (100) plane can be seen to shift to lower diffraction angles 28.27˚ with increases in calcination temperature.

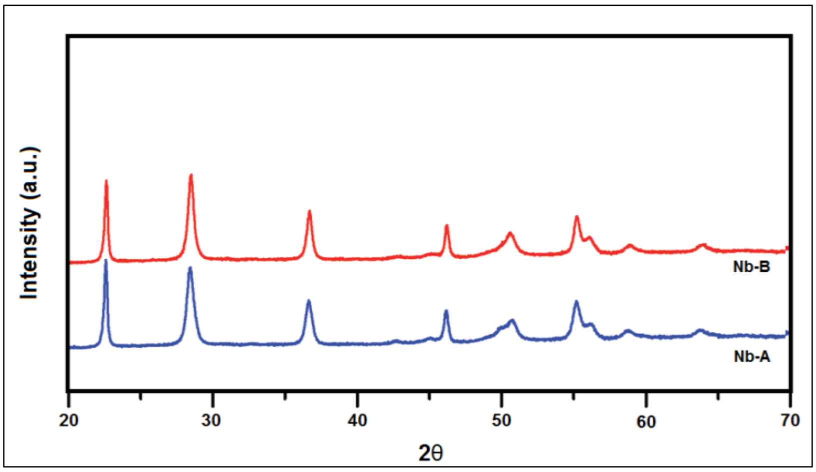

Figure 1 X-ray diffraction pattern of Nb_2O_5 at 450˚C (Nb-A) and 500˚C (Nb-B)

The main physicochemical properties of the niobium oxides are presented in Table 1. Average crystallite sizes of as synthesized Nb_2O_5 materials were calculated by the main diffraction signals observed at 2θ values of 28.52˚ and 28.27˚. The catalyst obtained at 450˚C display relatively large crystals although those of materials obtained at 500˚C are smaller.

Table 1: Main physicochemical parameters of as synthesized niobium oxide samples

Catalyst	**Calcination Temperature (˚C)**	**Lattice Parameters (Å)**			**Average Crystallite size (nm)**	**S_{BET} (m^2/g)**
		a	***b***	***c***		
Nb-A	450	3.6112	3.6112	3.9261	74.43	53.62
Nb-B	500	3.6119	3.6119	3.9269	33.21	67.45

3.2 Brunauer–Emmett–Teller (BET) surface area measurements

N_2 adsorption and desorption measurements were further performed on the prepared Nb_2O_5 samples to obtain the information of specific surface area and pore structure. From BET surface area measurements shown in Table 1, it could be concluded that the surface area of Nb_2O_5 was enhanced with increase in calcination temperature. Figure 2 depicts the nitrogen adsorption-desorption isotherms and the corresponding pore size distributions of Nb-A and Nb-B samples. From Figure 2 it can be seen that the adsorption-desorption isotherms of all three samples exhibit a type of IV-like behavior including a type H3 hysteresis loop according to the IUPAC classification. Such result demonstrated the existence of mesoporous structure in the prepared samples.

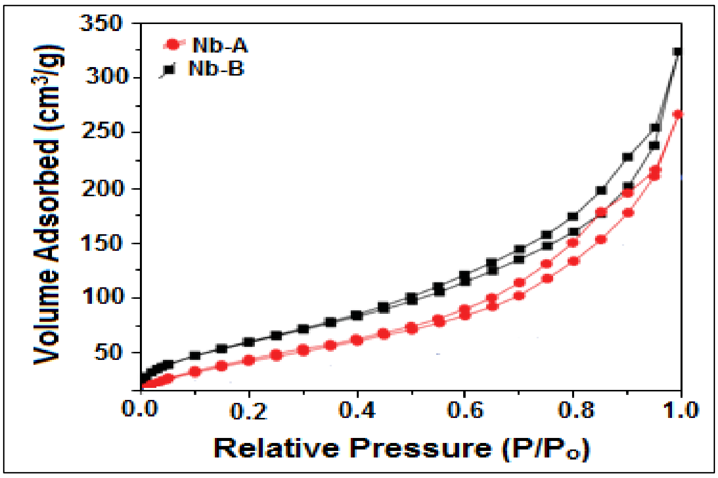

Figure 2: N_2 Adsorption-desorption isotherms of Nb-A and Nb-B samples

3.3 UV-Visible spectra

The UV-Vis absorption spectra of samples Nb-A and Nb-B are shown in Figure 3. As can be seen, both powder samples are transmittant in the visible range of the spectra above 400 nm. These results are in good agreement with our previous studies [13].

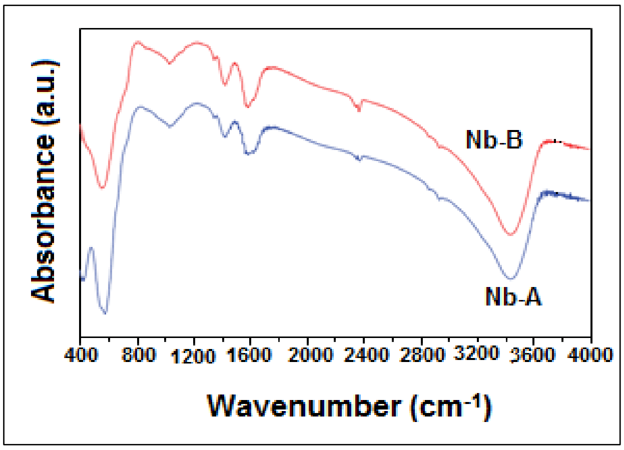

Figure 3: FT-IR spectra of synthesized Nb_2O_5 samples

3.4 FT-IR Analysis

The chemical-bond types of the as synthesized Nb2O5 samples were investigated by FT-IR. Figure 4 shows the typical FT-IR spectra of the prepared 4S, 6S, and 8S. From the FT-IR spectra, we can see that both the samples exhibit similar characteristics of infrared adsorption bands. Therein, the broad absorption peaks at 3420 and 1612 cm^{-1} can be ascribed to the vibration of absorptive water, and the absorption peaks at 576, 1098, and 1430 cm^{-1} are due to the vibration of Nb–O or Nb–O–Nb groups in Nb_2O_5. The results given by FT-IR analysis further confirm the formation of Nb_2O_5 materials and thus corroborate the results obtained in XRD analysis.

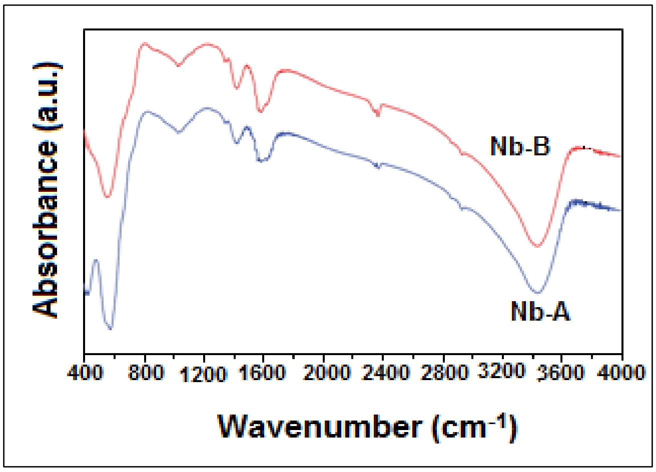

Figure 4: FT-IR spectra of synthesized Nb_2O_5 samples

3.5 Photocatalytic Activity

The photocatalytic performance of the Nb_2O_5 nanoparticles was tested by degrading RR yellow dye which was carried out in a photo-reactor. Here, the photocatalyst performance of sample Nb-B is only presented. Spectrometer was used to determine the concentration of RR yellow dye solution before and after the photocatalytic degradation every 20 min once.

3.5.1 Effect of Initial Dye Concentration

The effect of initial yellow RR dye concentration was studied over Nb_2O_5 photocatalysts under UV-light irradiation at constant catalyst loading and solution pH. The tested initial dye concentrations were 10-50 ppm in the presence of 1.0 g/L Nb_2O_5 and solution pH of 4. Figure 5 shows the degradation efficiency of RR dye as a function of initial dye concentration.

From the results, the degradation efficiency of yellow RR dye decreased as the initial dye concentration increased above 30 ppm. The degradation efficiency of dye determined at lower initial concentration of 30 ppm (89.3%) was much higher than those determined at 10 ppm (38.6%), 20 ppm (54.4%), 40 ppm (51.2) and 50 ppm (25.0 %). This trend of the result was also similar to the findings of Md. Bhuiyan *et al.*, [14]. At high concentration, photodegradation effeciency of photocatalyst falls dramatically. This is because, at higher dye concentration, dye molecules might adsorb on the catalyst surface and retards the significant interaction of UV light with photocatalyst molecules resulting in the decrease in the generation of hydroxyl radicals and hence the dye degradation [15]. Since the number of active radicals generated on the catalyst surface did not increase under the constant light intensity and irradiation time, there will be lesser active radicals to attack the dye molecules and led to lower degradation efficiency. Moreover, the decrease in the degradation efficiency at high concentrations could be due to the dye solution become more and more dense which can hinder the light from reaching the catalyst surface.

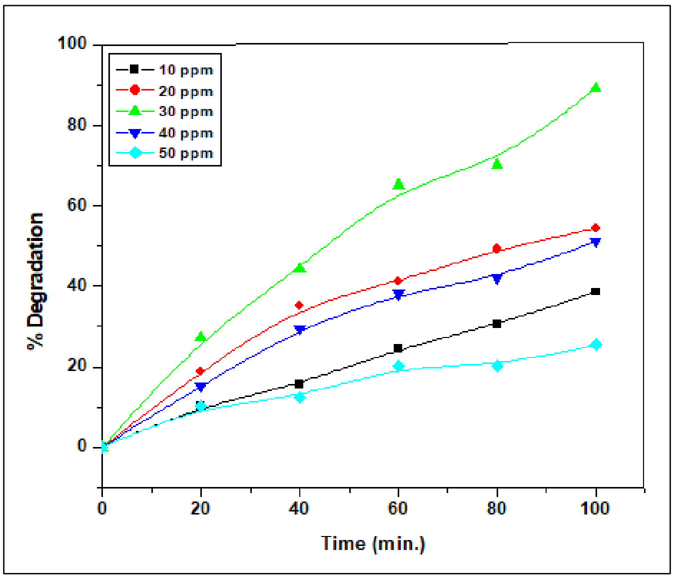

Figure 1: Effect of initial dye concentration on photodegradation of yellow RR dye [Conditions: Sample-Nb-B; Catalyst dose–1 g/L, pH-4].

3.5.2 Effect of Catalyst Loading

It was well known that catalyst loading has an effect on the photocatalytic degradation of organic pollutants. Thus, the effect of catalyst loading on the photocatalytic degradation of yellow RR dye over Nb_2O_5 photocatalysts under UV light irradiation was studied by varying the catalyst loading from 0.5 to 2.0 g/L at constant initial dye concentration (30 ppm) and solution pH (4). Figure 6 shows the degradation efficiency of dye as a function of photocatalyst loading. After 180 min of irradiation, the degradation efficiency of dye increased from 38.6% to 95.4% with increasing the catalyst loading from 0.5 to 1.5 g/L. However, at higher catalyst loading of 2.0 g/L, the degradation efficiency of dye decreased to 47.50%.

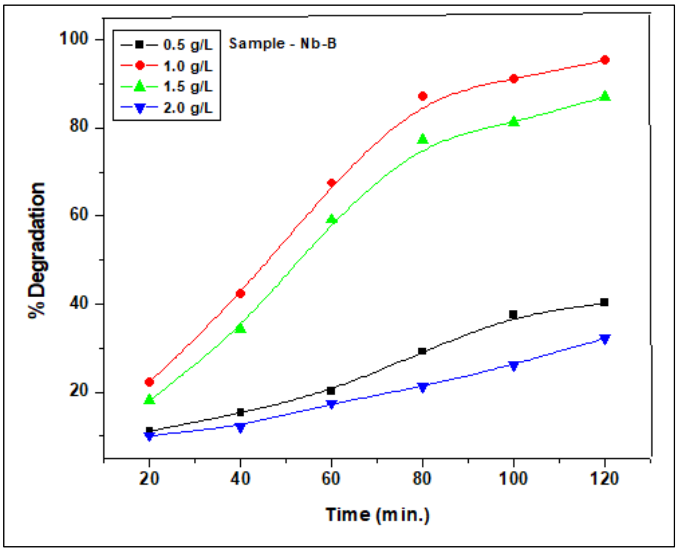

Figure 6: Effect of photocatalysts loading on the photocatalytic degradation of yellow RR dye [Initial dye concentration–30 ppm; pH-4]

The effect of catalyst loading on the dye degradation can be explained as the amount of catalyst increased, more catalyst active sites and higher adsorption area were available for the generation of active radicals for degradation of dye. As the catalyst loading increases beyond a certain amount, it leads to lower degradation efficiency because of the light scattering effect and increase in the particle aggregation

[15]. The excess of catalyst led to an increase in the turbidity of the suspension and consequently increased the light scattering effect. Thus, the light penetration decreased which resulted in lower degradation efficiency. In conclusion, based on the results obtained, optimum Nb_2O_5 loading was 1.5 g/L.

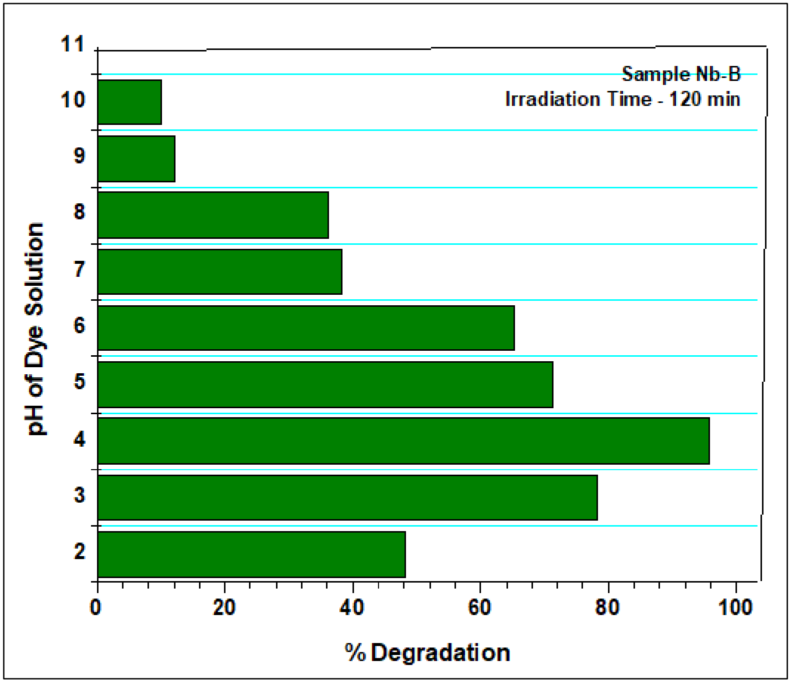

Figure 7: Effect of pH on photodegradation of yellow RR dye [Conditions: Initial dye concentration–30 ppm; Catalyst load-1.5 g/L].

3.5.3 Effect of pH

The influence of solution pH on the photocatalytic degradation of yellow RR dye over Nb_2O_5 photocatalysts under UV light irradiation are shown in Figure 7. A series of experiments was performed for sample Nb-B (1.5 g/L), initial dye concentration (30 ppm). The pH of the dye solution was adjusted in the range 2-10 before light irradiation and is not controlled during the degradation reaction. From Figure 7 it is clear that the degradation was favored at lower pH while it was found to be decreased with the increase in pH value. More specifically, the highest degradation of almost 95% was observed at pH 4, followed by 65% degradation at pH 5 while for the rest of the pH region the degradation almost remained same with the lowest value of about 10% within 120 min. The result indicates that acidic medium favour the photodegradation of yellow RR dye in presence of Nb_2O_5 catalyst.

The degradation of dye usually depends on the adsorption of dye molecules on the catalyst surface and formation of hydroxyl free-radical which in turn depends on the availability of hydroxyl ion in the reaction medium. The pH is the most important parameter for controlling the photocatalytic degradation of dyes, especially due to its effect on the catalyst surface. The pH_{pzc} value of the Nb_2O_5 catalyst reported by A. Nezamzadeh-Ejhieh was about 7.46 [16]. The Nb_2O_5 catalyst surface has the net zero charge at pH_{pzc} and at $pH < pH_{pzc}$ the surface of the catalyst is positively charged while at $pH > pH_{pzc}$ the surface is negatively charged.

3.5.4 Effect of oxidant species

In photocatalytic reaction the recombination of photogenerated electrons and holes is the cause of the low quantum yield of the process. The recombination electron/hole can be minimized by adding a proper electron acceptor to the system. Generally molecular oxygen (O_2), pure or in air, is used for this purpose. The addition of inorganic oxidants to the semiconductor suspension such as H_2O_2, $KClO_3$, $Na_2S_2O_8$, $KBrO_3$ and KIO_4 are recommended in order to compensate the oxygen deficiency caused either by consumption or slow oxygen mass transfer, [17, 18]. These compounds show a positive effect on the rate of the photocatalytic oxidation of organic molecules in water by avoiding electron/hole recombination, as they act as electron acceptors.

Hydrogen peroxide (H_2O_2) plays a dual role in photocatalytic reaction acting as electron acceptor (Eq. I), promoting the charge separation, being also able to decompose to produce HO• radicals by absorption of light (eq. II). The effect of H_2O_2 addition in photodegaration of RB5 dye over Nb_2O_5 photocatalyst was reported in earlier studies [14]. In the present study, hydrogen peroxide and was tested as oxidizing agents in the photodegradation of yellow RR dye. From Figure 7, it can be depicted that the addition of H_2O_2 to Nb_2O_5 suspensions produced a significant enhancement on the photodegradation of yellow RR dye in 40 min of light irradiation.

$H_2O_2 + e^- \rightarrow HO\bullet + HO^-$ ………………. (I)

$H_2O_2 \xrightarrow{hv} 2HO\bullet$ ……………………… (II)

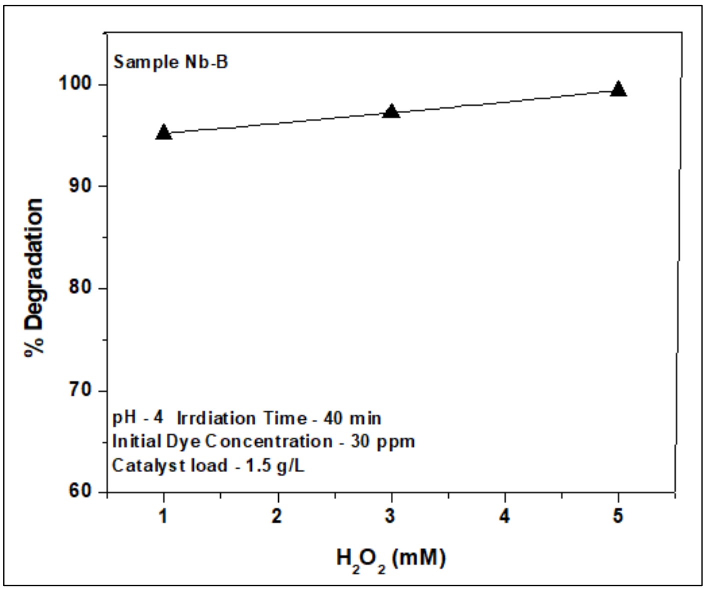

Figure 7: Effect of H_2O_2 addition on photodegaration of yellow RR dye

3.5.5 Scavenger Test

Many former investigations well-documented that active species including holes (h_{vb}^+), hydroxyl radicals (•OH) and super oxide anion radicals ($O_2\bullet^-$) were involved in photocatalysis [19-21]. In the present investigation, ethanol was added as a scavenger of •OH radicals and sodium oxalate was used to scavenge h_{vb}^+ due to its efficient formation of CO_2 and $CO_2\bullet^-$ as in the reaction sequence shown below [22]. Ethanol has been generally used as •OH radicals scavenger to estimate the oxidation mechanism due to its high rate constant of reaction between •OH radicals and ethanol [23].

$C_2O_4^{2-} \xrightarrow{hv} CO_2 + CO_2\bullet$ ………………. (III)

Figure 8, shows the effect of scavengers (2mM) on photodegaration of yellow RR dye. From figure 8, one can see that by addition of ethanol and sodium oxalate scavengers the degradation of dye decreases from 95% to 45.2% and 21.2% respectively.

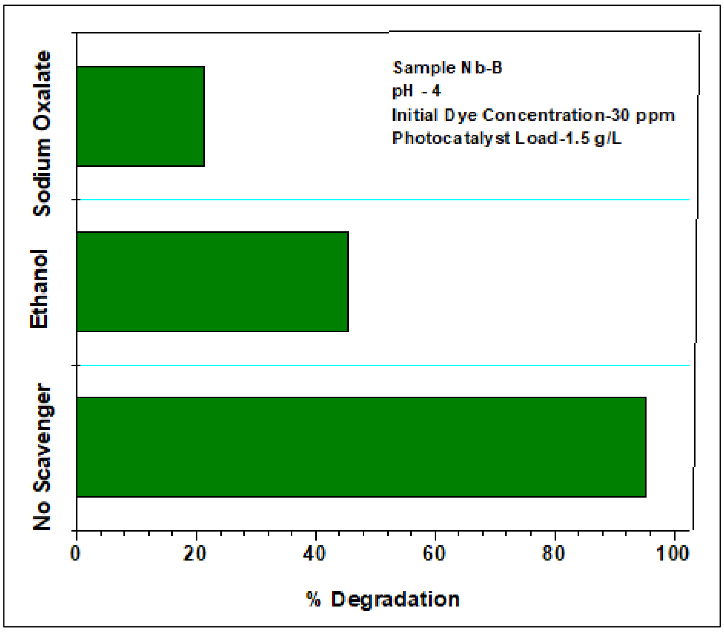

Figure 8: Effect of different scavengers at 2 mM on photocatalytic degradation of Remazol yellow RR dye dye Nb_2O_5 photocatalysts

3.5.6 Reusability of photocatalyst

Figure 9 shows the reusability of the Nb-B catalyst for the degradation of Remazol yellow RR dye. After five cycles the catalyst could degrade the dye by 95% for catalyst dose 1.5 g/L, initial dye concentration 30 ppm in 120 min at pH 4. The activity was found to decrease by 25.0% compared to the fresh catalyst.

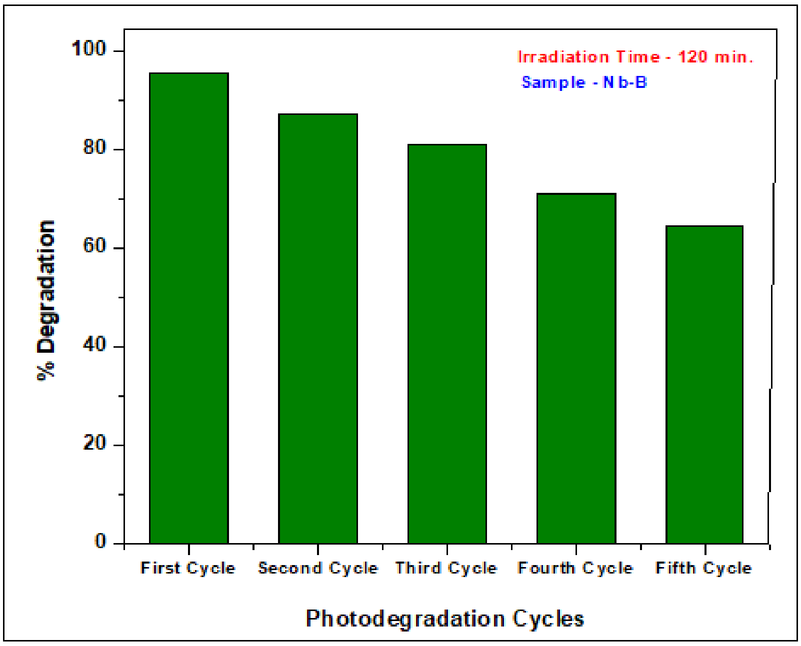

Figure 9: Reusability of Nb_2O_5 photocatalyst for degradation of RR dye [Conditions: Initial dye concentration–30 ppm; Catalyst load-1.5 g/L, pH-4].

The calculated BET surface areas for Nb-A and Nb-B samples were found to be 53.62 and 67.45 m^2/g respectively. Obviously, the surface area of Nb-B was higher than that of NB-A. Combined with the TEM analysis, it can be concluded that the surface area of the prepared samples seriously increased with the increasing of crystal size of with calcination temperature.

4. CONCLUSION

The Nb_2O_5 nanoparticles with different surface area and particle size were synthesized by effectively through a green synthesis route by using the Aloe Vera gel. The crystallite size of the Nb_2O_5 photocatalyst estimated was in the range of 30-75 nm with large specific surface area ranging from 53-67 m^2/g. Physicochemical characterization of as-prepared Nb_2O_5 was carried out with help of XRD, EDAX, FTIR and UV–Visible spectroscopy. Further, photocatalytic activities of Nb_2O_5 nanoparticles have been investigated by photocatalytic degradation of organic dye yellow RR dye in the presence of UV light and about 95% of 30 ppm dye at pH 4 for 1.5 g/L of Nb-B photocatalyst. Therefore, Nb_2O_5 is a promising catalyst for the degradation of dyes and further research is needed to improve the research scope in development of Nb_2O_5 based photocatalyst for visible light driven reactions.

REFERENCES

1. Pawar, M., Topcu Sendoğdular, S., & Gouma, P. (2018). A brief overview of TiO2 photocatalyst for organic dye remediation: case study of reaction mechanisms involved in Ce-TiO2 photocatalysts system. *Journal of Nanomaterials*, *2018*, 1-13.
2. Nagappan, S., Lee, D. B., Seo, D. J., Park, S. S., & Ha, C. S. (2015). Superhydrophobic mesoporous material as a pH-sensitive organic dye adsorbent. *Journal of Industrial and Engineering Chemistry*, *22*, 288-295.
3. Thebo, K. H., Qian, X., Zhang, Q., Chen, L., Cheng, H. M., & Ren, W. (2018). Highly stable graphene-oxide-based membranes with superior permeability. *Nature communications*, *9*(1), 1486-1493.
4. Jung, K. W., Choi, B. H., Dao, C. M., Lee, Y. J., Choi, J. W., Ahn, K. H., & Lee, S. H. (2018). Aluminum carboxylate-based metal organic frameworks for effective adsorption of anionic azo dyes from aqueous media. *Journal of industrial and engineering chemistry*, *59*, 149-159.
5. Iqbal, M., Ali, A., Nahyoon, N. A., Majeed, A., Pothu, R., Phulpoto, S., & Thebo, K. H. (2019). Photocatalytic degradation of organic pollutant with nanosized cadmium sulfide. *Materials Science for Energy Technologies*, *2*(1), 41-45.
6. Zhang, H., Wang, Y., Liu, P., Chou, S. L., Wang, J. Z., Liu, H., ... & Zhao, H. (2016). Highly ordered single crystalline nanowire array assembled three-

dimensional Nb3O7 (OH) and Nb2O5 superstructures for energy storage and conversion applications. *ACS nano*, *10*(1), 507-514.

7. Yan, W., Zhang, G., Yan, H., Liu, Y., Chen, X., Feng, X., ... & Yang, C. (2018). Liquid-phase epoxidation of light olefins over W and Nb nanocatalysts. *ACS Sustainable Chemistry & Engineering*, *6*(4), 4423-4452.
8. Liang, F., & Liu, J. (2017). Sintering, microstructure and electricity properties of ITO targets with Bi2O3–Nb2O5 addition. *Ceramics International*, *43*(8), 5856-5861.
9. Zarrin, S., & Heshmatpour, F. (2018). Photocatalytic activity of TiO2/Nb2O5/PANI and TiO2/Nb2O5/RGO as new nanocomposites for degradation of organic pollutants. *Journal of hazardous materials*, *351*, 147-159.
10. Li, S., Wang, T., Zhu, W., Lian, J., Huang, Y., Yu, Y. Y., ... & Li, H. (2019). Controllable synthesis of uniform mesoporous H-Nb 2 O 5/rGO nanocomposites for advanced lithium ion hybrid supercapacitors. *Journal of Materials Chemistry A*, *7*(2), 693-703.
11. Lopes, O. F., Paris, E. C., & Ribeiro, C. (2014). Synthesis of Nb2O5 nanoparticles through the oxidant peroxide method applied to organic pollutant photodegradation: A mechanistic study. *Applied Catalysis B: Environmental*, *144*, 800-808.
12. Izadiyan, Z., Shameli, K., Miyake, M., Hara, H., Mohamad, S. E. B., Kalantari, K., ... & Rasouli, E. (2020). Cytotoxicity assay of plant-mediated synthesized iron oxide nanoparticles using Juglans regia green husk extract. *Arabian Journal of Chemistry*, *13*(1), 2011-2023.
13. Pawar, M. J., & Gaonar, M. D. (2022). “Photodegradation of Reactive Black 5 Azo dye (RB5) By Nb_2O_5 Photocatalyst Synthesized by Modified Sol-gel Method”, *International Journal of Chemical Studies*, 10(3), 22-26.
14. Bhuiyan, M. S. H., Miah, M. Y., Paul, S. C., Aka, T. D., Saha, O., Rahaman, M. M., ... & Ashaduzzaman, M. (2020). Green synthesis of iron oxide nanoparticle using Carica papaya leaf extract: application for photocatalytic degradation of remazol yellow RR dye and antibacterial activity. *Heliyon*, *6*(8), e04603.
15. Chen, C., Liu, J., Liu, P., & Yu, B. (2011). Investigation of photocatalytic degradation of methyl orange by using nano-sized ZnO catalysts. *Advances in Chemical Engineering and Science*, *1*(1), 9-14.
16. Nezamzadeh-Ejhieh, A., & Bahrami, M. (2015). Investigation of the photocatalytic activity of supported ZnO–TiO2 on clinoptilolite nano-particles towards photodegradation of wastewater-contained phenol. *Desalination and Water Treatment*, *55*(4), 1096-1104.
17. Figueiredo, J. L., Pereira, M. F., Freitas, M. M., & Órfão, J. J. (2007). Characterization of active sites on carbon catalysts. *Industrial & Engineering Chemistry Research*, *46*(12), 4110-4115.
18. Chen, L., Zhang, B. L., Qu, M. Z., & Yu, Z. L. (2005). Preparation and characterization of CNTs–TiO2 composites. *Powder Technology*, *154*(1), 70-72.
19. Ahmed, S., Rasul, M. G., Martens, W. N., Brown, R., & Hashib, M. A. (2010). Heterogeneous photocatalytic degradation of phenols in wastewater: a review on current status and developments. *Desalination*, *261*(1-2), 3-18.
20. Lam, S. M., Sin, J. C., Abdullah, A. Z., & Mohamed, A. R. (2012). Degradation of wastewaters containing organic dyes photocatalysed by zinc oxide: a review. *Desalination and Water Treatment*, *41*(1-3), 131-169.
21. Ribeiro, A. R., Nunes, O. C., Pereira, M. F., & Silva, A. M. (2015). An overview on the advanced oxidation processes applied for the treatment of water pollutants defined in the recently launched Directive 2013/39/EU. *Environment international*, *75*, 33-51.
22. Wang, W., Huang, G., Jimmy, C. Y., & Wong, P. K. (2015). Advances in photocatalytic disinfection of bacteria: development of photocatalysts and mechanisms. *Journal of Environmental Sciences*, *34*, 232-247.
23. Xian, T., Yang, H., Di, L., Ma, J., Zhang, H., & Dai, J. (2014). Photocatalytic reduction synthesis of $SrTiO_3$-graphene nanocomposites and their enhanced photocatalytic activity. *Nanoscale Res Lett*, 9(1), 327-330.

Cite This Article: M. J. Pawar, M. D. Gaonar, A. D. Khajone, P. R. Malasane (2023). Green Synthesis of Nb_2O_5 Nanoparticles and Photodegradation of Remazol Yellow RR Dye. *East African Scholars Multidiscip Bull, 6*(1), 1-9.